PHYSICAL REVIEW B VOLUME 39, NUMBER 2 15 JANUARY 1989-I

Resonance photoemission at the 2*p* excitation threshold of Ni{001}

S. C. Wu,* C. K. C. Lok, J. Sokolov,† and F. Jona
College of Engineering and Applied Science, State University of New York, Stony Brook, New York 11794

A. Taleb-Ibrahimi
IBM Research Center, Yorktown Heights, New York 10598

(Received 20 June 1988)

Resonance enhancement of the 3*d* photoemission intensity in angle-integrated electron-distribution curves from Ni{001} is observed when the photon energy is varied in the vicinity of the Ni 2*p* absorption threshold. Explanation of the effect involves a Fano-like interference between continuum excitation from the 3*d* band and discrete excitation from the 2*p* level to form a core exciton, coupled to each other via the decay of the exciton and the ejection of a 3*d* electron into the continuum. The binding energy of the core exciton is about 3.5 eV below the absorption threshold. Differences between the $2p \rightarrow 3d$ and the well-known $3p \rightarrow 3d$ resonance effect are discussed.

I. INTRODUCTION

Resonance photoemission was discovered in Ni metal by Guillot *et al.*[1] in 1977 and was frequently discussed in the literature from the theoretical point of view.[2–5] The phenomenon consists of a dramatic increase of a photoemission peak located about 6 eV below the Fermi level when the photon energy is varied through the Ni 3*p* threshold at about 67 eV. The phenomenon was attributed to an interference effect formally similar to that described by Fano[6] in his treatment of the energy-loss spectrum of He. In the case of the Ni resonance the interference is between the excitation of a 3*p* electron to the empty part of the *d* band (core exciton, $3p^63d^94s \rightarrow 3p^53d^{10}4s$) and the excitation of 3*d* electrons into the continuum ($3p^63d^94s \rightarrow 3p^63d^84s\ \epsilon l$), coupled to each other via the decay of the exciton and the ejection of a 3*d* electron into the continuum (super-Koster-Kronig decay, $3p^53d^{10}4s \rightarrow 3p^63d^84s\ \epsilon l$). Barth *et al.*[7] demonstrated that not only the 6-eV peak but also the 3*d*-band photoemission is coupled to the 3*p* excitation at threshold. The latter interaction is weaker, to be sure, since the intensity variation is much smaller than for the 6-eV peak, but the valence-band emission is enhanced over a photon-energy range of about 30 eV. Furthermore, the $3p \rightarrow 3d$ interaction is not the same for the whole *d* band but rather differs from the top to the bottom of the band. Dietz *et al.*[8] showed that similar Fano interferences are responsible for the line shapes of core-excitation edges in Ni, Cu, Pt, and Au. Resonance photoemission was also observed in Cr, Fe, and Co,[9] but was disputed by Raaen *et al*,[10] who failed to see the effect in freshly evaporated thin films and therefore concluded that the earlier observations were caused by trace amounts of impurities in the samples used.

The interest in extending the study of resonance photoemission from the 3*p* to the 2*p* excitation threshold is twofold. First, there is the question of whether a core exciton can exist at the 2*p* absorption threshold of Ni. Second, if such an exciton exists one wonders what effects will be associated with its decay. The expectation is that the resonance phenomenon, if it occurs, will be different from the 3*p* case because the overlap of the 2*p* core exciton with the 3*d* wave function is much smaller than that of the 3*p* exciton. We recall that direct evidence of the latter was provided by the resonance enhancement of the oxygen 2*p* level in an oxygen-covered Ni_3Al\{001\} surface, an effect due to the overlap of the core exciton with the oxygen 2*p* wave function.[11] We present below some experimental results that demonstrate the existence of a resonance phenomenon at the Ni 2*p* absorption threshold. The phenomenon involves no satellite peaks below the 3*d* valence band, but rather the 3*d* band itself. The binding energy of the 2*p* core exciton is markedly larger (about 3.5 eV) than that of the 3*p* core exciton.

II. EXPERIMENTS

The experiments were performed at beam line U8 of the National Synchrotron Light Source (NSLS) at Brookhaven National Laboratory. The synchrotron light was dispersed by a 10-m toroidal-grating monochromator[12] and the photoelectron energies were measured with a two-dimensional display-type spectrometer[13] operated in an angle-integrated mode. The samples used in the experiments were a Ni{001} and an Fe{001} platelet, cleaned *in situ* by means of argon-ion bombardments and then annealed at about 800 °C. Photoemission spectra revealed no S, C, or O impurities, and low-energy electron diffraction patterns confirmed good long-range order on the surfaces.

The absorption spectra in the region of the *L* edges were measured for both samples by monitoring the integrated current of secondary electrons in the range from 0 to 5 eV. Both spectra are shown in Fig. 1. Angle-integrated electron-distribution curves (EDC's) from Ni{001} were measured and normalized to constant incident photon flux for a number of photon energies in the vicinity of the 2*p* edge (847.5 eV). Some of these EDC's are depicted in Fig. 2. There is no resonance enhance-

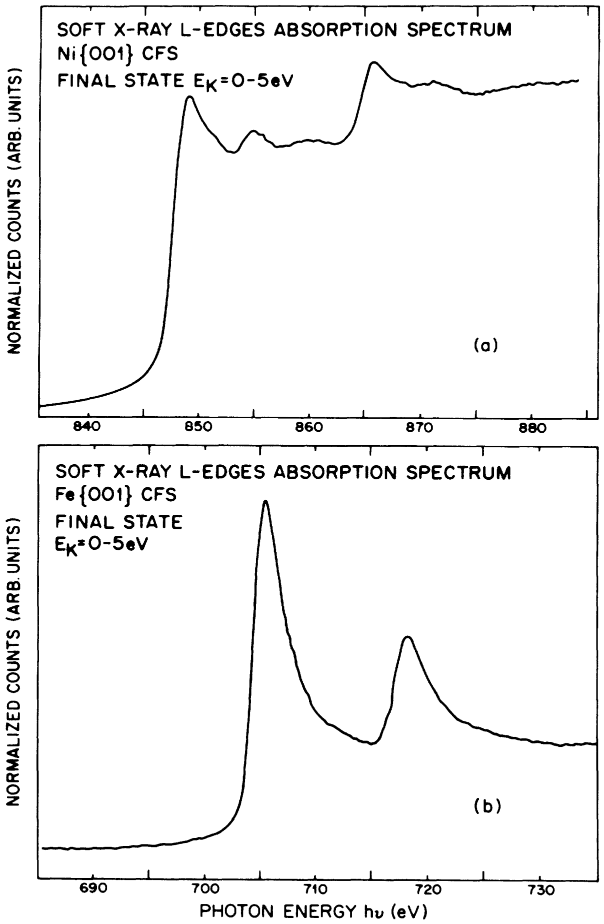

FIG. 1. Soft-x-ray L-edge absorption spectra of (a) Ni and (b) Fe.

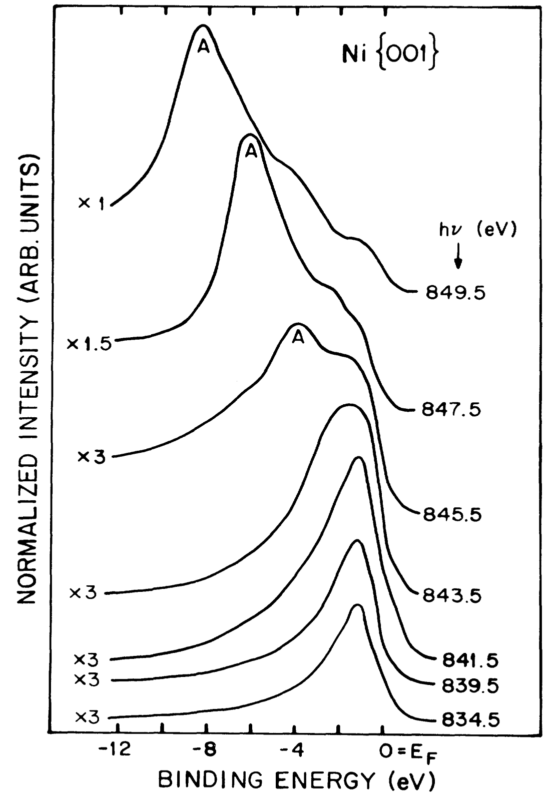

FIG. 2. Angle-integrated electron-distribution curves from Ni{001} for photon energies $h\nu$ as indicated.

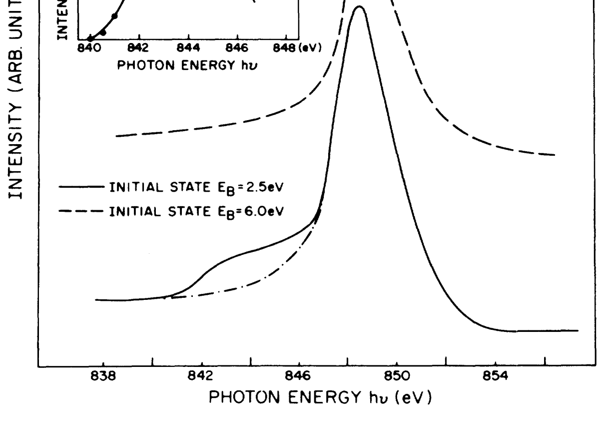

FIG. 3. Constant-initial-state (CIS) spectra from Ni{001}: solid curve for initial state 2.5- eV below the Fermi level E_F, dashed curve for initial state 6 eV below E_F. Inset shows the difference between the 2.5- and the 6-eV curves.

ment around 6 eV below the Fermi level E_F, but the intensity of the $3d$ peak (from 0 to 3 eV below E_F) increases markedly when the photon energy approaches the $2p$ absorption threshold, and reaches a maximum at about 843.5 eV, about 4 eV below the Ni $2p$ absorption threshold (847.5 eV). This resonance phenomenon is accompanied by the appearance of a well-characterized Auger transition ($L_3M_{4,5}N_{4,5}$) indicated with the letter A in Fig. 2. The Auger peak is much larger than the $3d$ peak because the ionization cross section of the $2p$ level is about 1.5 orders of magnitude larger than the ionization cross section of the $3d$ band.[14]

In order to examine in more detail the photoemission intensity in the photon-energy range around the $2p$ absorption edge, we have measured constant-initial-state (CIS) spectra. Such spectra are obtained by synchronously sweeping the photon energy with the transmission-energy window (1 eV wide) of the analyzer, so that the energy of the initial state is kept constant. Figure 3 depicts two such CIS spectra, one for the initial state at 2.5 eV, the other for the initial state at 6 eV below E_F. Both curves exhibit a very large peak which arises from the Auger transition mentioned above (peak A in Fig. 2). The 2.5-eV curve also shows a small but detectable shoulder on the lower-photon-energy side. We can subtract the Auger contribution in this energy range by assuming that the shape of the Auger peak does not change from 6 to 2.5 eV (dashed-dotted curve in Fig. 3). The inset in Fig. 3 depicts the difference between the two curves, which reaches a maximum at a photon energy of 844 eV. This result is consistent with the resonance enhancement of the 3*d* peak shown in Fig. 2. The shoulder in the CIS curve is much smaller than the height of the Auger peak because the excitation cross section of the 2*p* core exciton is much smaller than the ionization cross section of the 2*p* level. The binding energy of the exciton state can be estimated by comparing the inset in Fig. 3 with the absorption curve in Fig. 1(a), which exhibits the edge at 847.5 eV. Thus, the binding energy of the excitation associated with the resonance is 3.5 eV.

III. DISCUSSION

There are two main differences between the resonance photoemission associated with the $2p \rightarrow 3d$ excitation and that caused by the $3p \rightarrow 3d$ excitation.

(i) Around the 3*p* threshold most of the enhancement in photoemission intensity occurs in the region of the 6-eV satellite, although the valence-band emission is also enhanced, but to a lesser degree and over a broader energy range of about 30 eV, with a sharp dip at the 3*p* threshold itself.[7] By contrast, at the 2*p* threshold no resonance satellites are observed below the valence band, but the main peak of the 3*d* band exhibits a pronounced resonance behavior. To understand this difference we need to scrutinize the possible excitation steps in the two cases.

In Fig. 4(b) we show a schematic diagram of the photoemission from the 3*d* band, which has a continuous excitation spectrum. Figure 4(c) shows a so-called direct recombination process. Absorption of a photon raises an electron from the 3*p* to the empty part of the 3*d* band, thus creating a hole in the 3*p* band and a conduction electron in the 3*d* band. When this electron-hole pair (exciton) recombines, the liberated energy is transferred to a valence electron, which is ejected. Thus the final state consists of a free electron and a core hole. The kinetic energy of the free electron is determined by the initial state with binding energy E_b in the 3*d* valence band. A Fano-type interference between the continuous excitation of Fig. 4(b) and the discrete excitation of Fig. 4(c) gives rise to the observed resonance effect.

There is another possible decay mechanism for the exciton, a mechanism similar to Auger decay. A valence electron recombines with the core hole and the liberated energy ejects another valence electron into vacuum, leaving the original conduction electron at the Fermi surface [Fig. 4(d)]. Thus, the final state consists of a free electron and *two* holes in the valence band. Penn[2] has shown that these two *d* holes are correlated in such a way that there is a relatively high probability that they are located in the same atom, resulting in a $3d^8$ configuration. At the Ni 3*p* threshold the exciton decay occurs predominantly via the Auger-like process depicted in Fig. 4(d), and if the resulting two *d* holes are left in a virtual bound state, then the ejected electron has an energy corresponding to the satellite, thus contributing to the enhancement of the latter's intensity at resonance.

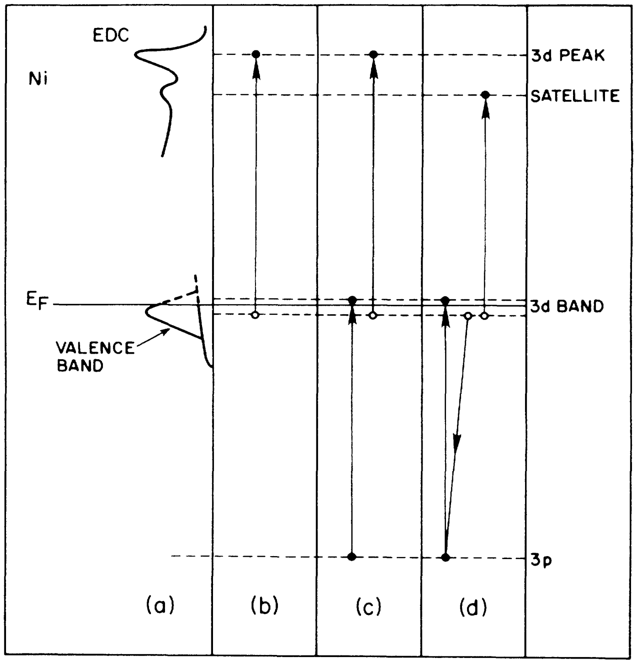

FIG. 4. Schematic representation of the photoionization processes involved in the resonance photoemission in Ni: (a) occupied density of initial states below the Fermi level and sketch of the valence-band spectrum at resonance; (b) continuum excitation, single-hole final state; (c) discrete excitation, single-hole final state; (d) discrete excitation, double-hole final state. [Adapted from M. R. Thuler, R. L. Benbow, and Z. Hurych, Phys. Rev. B **27**, 2082 (1983).]

The situation is different at the 2*p* threshold. In this case the excited electron is bound to a 2*p*-core hole. Since the overlap of the 3*d* wave function with the 2*p*-hole wave function is much smaller than that with the 3*p*-hole wave function, the decay of the well-localized discrete excitation state occurs predominantly by way of a direct recombination process such as that depicted in Fig. 4(c), rather than by way of the Auger-type decay shown in Fig. 4(d). It is for this reason that the 2*p* excitation does not produce a satellite resonance, but rather a 3*d* valence-band photoemission enhancement.

(ii) The second main difference between the 3*p* and the 2*p* resonance lies in the binding energies of the corresponding core excitons. In the 3*p* case the resonance energy (i.e., the energy at maximum intensity of the 6-eV satellite peak) is very close (within 0.1 eV) to the 3*p* absorption threshold. In the 2*p* case the resonance energy, as obtained from the CIS spectra in Fig. 3, is about 3.5 eV smaller than that of the absorption threshold. Thus, the binding energy of the 2*p*-core exciton (about 3.5 eV) is much larger than that of the 3*p*-core exciton (less than 0.1 eV), and therefore there must be a discrete excitation state about 3.5 eV below the 2*p* absorption edge. However, such a discrete state is not immediately visible in the absorption spectrum depicted in Fig. 1(a). There are three reasons for this fact: (1) the intensity of the exciton peak is much smaller than that of the 2p absorption edge (the ionization cross section of the 2p level is much larger than the exciton cross section); (2) the experimental energy resolution (about 1 eV) smears out the exciton level; (3) lifetime effects may broaden the exciton level. Nevertheless, the presence of this level in the absorption curve can be revealed by an indirect procedure, which we describe in the following.

We argue that if the exciton level were not present, then the Ni 2p absorption curve would lie well below the measured curve of Fig. 1(a) in the region below the edge. To prove this point we would like to construct the absorption curve of a fictitious Ni crystal which does *not* have the 2p exciton level (we will call it, for short, the "fictitious" curve). We show below that we can get information about such a "fictitious" curve by suitably modifying the absorption curve of a crystal of Fe. Fe is a good candidate for this purpose because its 2p threshold is energetically near that of Ni, the natural width of its 2p level is larger than that of Ni,[15] and no exciton level is known to exist below this threshold. We will in fact assume that no such level exists.[16] The 2p absorption curve for Fe is shown in Fig. 1(b).

Before we proceed with the modification of the Fe curve, we want to recall that any absorption curve, at and below the absorption edge, results from a convolution of a steplike function $S(E)$ with a Gaussian-Lorentzian broadening function $B(E)$. (Above the absorption edge, the shape of the curve is controlled by the density of unoccupied states above the Fermi level.) The broadening function $B(E)$ is itself a convolution between a Gaussian instrumental broadening function $G(E)$ [with full width at half maximum (FWHM) ΔE_G] and a Lorentzian level line-shape function $L(E)$ (with FWHM ΔE_L). The slope of the absorption curve near the edge is dominated by the instrumental resolution (ΔE_G), whereas the shape of the absorption curve in the tail below the edge is governed predominantly by the natural width of the core level (ΔE_L). If both the instrumental and the natural width were multiplied with the same factor, so that the Gaussian-Lorentzian mixing ratio $\Delta E_G/\Delta E_L$ remains fixed, then the shape of the *normalized* broadening function would not change, although the abscissa (i.e., energy) values of the corresponding absorption curve below the edge would be multiplied by the same factor. In the present case, if both instrumental resolution and the natural level width of Fe and Ni were the same, then the Fe absorption curve could safely be assumed to have the shape of the "fictitious" curve that we are seeking. However, the 2p natural width is smaller for Ni than for Fe,[15] and the instrumental resolution is worse at the Ni edge than at the Fe edge. The latter fact is confirmed by the observation that at the edge the slope of the Ni curve is smaller than that of the Fe curve (Fig. 1). Now, if we assume that the natural width of the Ni 2p level is *increased* by the same factor as the ratio of the instrumental broadenings for Ni and Fe, i.e., we keep the ratio $\Delta E_G/\Delta E_L$ constant, then we can "correct" the Fe curve to provide an upper bound for the "fictitious" curve that we are seeking.

The correction of the Fe curve is done as follows. First, we normalize the Fe and Ni curves by equating to one another, respectively, the background values well below (13 eV) the edges and at the midpoints of the edges themselves (Fig. 5). Second, we determine the slopes s_{Ni} and s_{Fe} of the normalized curves at the middle points and their ratio $s_{\mathrm{Ni}}/s_{\mathrm{Fe}}$. This ratio, as mentioned above, represents essentially the ratio of the instrumental broadenings at the two edges. Third, starting from the Fe curve we calculate, point by point, a new curve for which the abscissa (i.e., the energy) values below the edge increase by the ratio $s_{\mathrm{Ni}}/s_{\mathrm{Fe}}$, i.e., referring to Fig. 5, $OB = OA\,(s_{\mathrm{Ni}}/s_{\mathrm{Fe}})$. This new curve represents what the Fe absorption curve would look like if it had been measured with the same poorer resolution that prevails at the Ni edge. This new curve is an upper bound of the "fictitious" curve that we want because it involves the larger

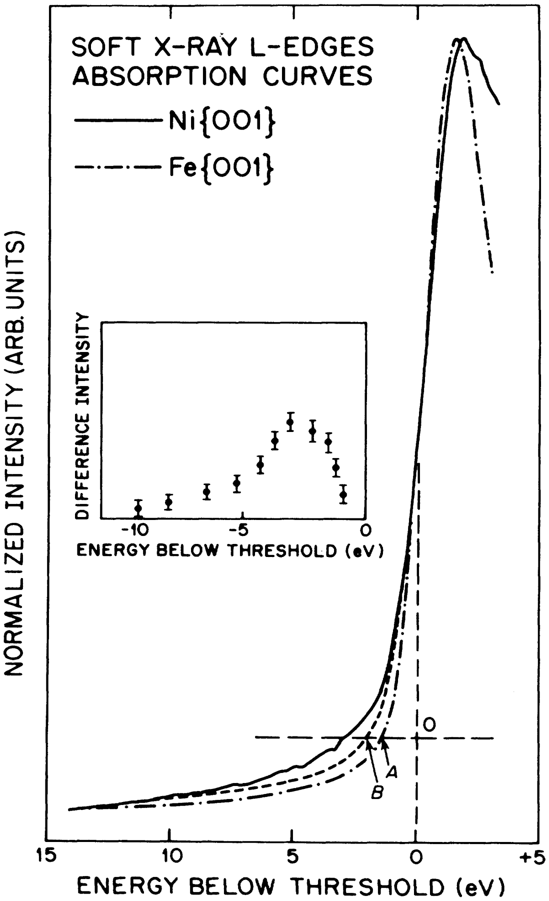

FIG. 5. Normalized Ni and Fe L edges. The dashed curve was calculated point by point from the Fe curve by first measuring the latter's abscissa values from the edge (e.g., OA) and then calculating the new abscissa values (e.g., OB) as described in the text. The dashed curve is an upper bound for the absorption curve of a fictitious Ni crystal which has no exciton state below the 2p edge. The inset shows the difference between the Ni and the dashed curve.

natural level width of the Fe curve, whereas the "fictitious" curve would involve the smaller Ni $2p$ width. Thus, such a "fictitious" curve (the absorption curve of a fictitious Ni crystal *without* the exciton state) would lie *below* the dashed curve. The experimental curve of real Ni, as shown in Fig. 5, lies well above the upper-bound curve, proving that there is a discrete excitation level just about 3.5±0.5 eV below the $2p$ absorption threshold. This conclusion is, of course, consistent with the photoemission results presented above.

Perhaps most surprising is the fact that this exciton state has such a large binding energy as compared to the $3p$ counterpart. A satisfactory explanation is not available at the present time, but a possible explanation suggests itself on the basis of theoretical results of Davis and Feldkamp.[17] These authors studied the effect of electron correlations on the photoemission from narrow-band metals, and explained, among other things, the appearance of the small satellite observed about 6 eV below the $2p$ peak in the photoemission spectrum of Ni. In Ni, where the electron correlation energy in the d band is much larger than the bandwidth, the interaction between a $2p$ hole and the $3d$ band produces a new bound state just below the bottom of the $3d$ band. When this level is occupied the photoemission spectrum exhibits the main $2p$ peak, but when this level is unoccupied (owing to excitation into the empty part of the $3d$ band) the spectrum exhibits a satellite peak at larger binding energy (reflecting the decrease in kinetic energy of the ejected $2p$ electron). Now, if there is a finite probability that the bound state produced by the $2p$-hole–$3d$-band interaction is unoccupied, and if a transition from the $2p$ level to this bound state is allowed, thus creating an exciton, then one may be able to explain the observations reported in this paper.

ACKNOWLEDGMENT

This work was supported in part by National Science Foundation Grant No. DMR-87-09021.

---

[*] On leave from the Department of Physics, Peking University, Beijing, The People's Republic of China.

[†] On leave from the Weizmann Institute of Science, Rehovot, Israel.

[1] C. Guillot, Y. Ballu, J. Paigné, J. Lecante, K. P. Jain, P. Thiry, R. Pinchaux, Y. Petroff, and L. M. Falicov, Phys. Rev. Lett. **39**, 1632 (1977).

[2] D. R. Penn, Phys. Rev. Lett. **42**, 921 (1979).

[3] A. Liebsch, Phys. Rev. Lett. **43**, 143 (1979).

[4] L. C. Davis and L. A. Feldkamp, Phys. Rev. B **23**, 6239 (1981).

[5] N. Martensson and B. Johansson, Phys. Rev. Lett. **45**, 482 (1980).

[6] U. Fano, Phys. Rev. **124**, 1866 (1961).

[7] J. Barth, G. Kalkoffen, and C. Kunz, Phys. Lett. **74A**, 360 (1979).

[8] R. Dietz, E. McRae, and J. Weaver, Phys. Rev. B **21**, 2229 (1980).

[9] D. Chandesris, J. Lecante, and Y. Petroff, Phys. Rev. B **27**, 2630 (1983), and references cited therein.

[10] S. Raaen, V. Murgai, and X. Q. Yang, National Synchrotron Light Source (NSLS) Annual Report, 1986, p. 215 (unpublished).

[11] S. C. Wu, Z. Q. Wang, R. F. Garrett, D. Sondericker, J. Sokolov, and F. Jona, Europhys. Lett. **1**, 655 (1986).

[12] F. J. Himpsel, Y. Jugnet, D. E. Eastman, J. J. Donelon, D. Grimm, G. Landgren, A. Marx, J. F. Morar, C. Oden, R. A. Pollak, and J. Schneir, Nucl. Instrum. Methods **222**, 107 (1984).

[13] D. E. Eastman, J. J. Donelon, N. C. Hien, and F. J. Himpsel, Nucl. Instrum. Methods **172**, 327 (1980).

[14] J. J. Yeh and I. Lindau, At. Data Nucl. Data Tables **32**, 48 (1985).

[15] C. O. Wagner, W. M. Riggs, L. E. Davis, J. F. Moulder, and G. E. Mailenberg, *Handbook of X-Ray Photoelectron Spectroscopy* (Perkin-Elmer, Eden Prairie, 1979), pp. 76 and 82.

[16] Even if there were an exciton state below the Fe $2p$ threshold, this fact would not invalidate the argument developed below about the existence of a Ni $2p$ exciton.

[17] L. C. Davis and L. A. Feldkamp, J. Appl. Phys. **50**, 944 (1979).